Optimal yaw strategy for optimized power and load in various wake situations

Paper

Urban, Albert M.; Larsen, Torben J.; Larsen, Gunner Chr.; Held, Dominique P.; Dellwik, Ebba; Verelst, David Robert

Published in:
Journal of Physics: Conference Series

Link to article, DOI:
10.1088/1742-6596/1102/1/012019

Publication date:
2018

Document Version
Publisher's PDF, also known as Version of record

Optimal yaw strategy for optimized power and load in various wake situations

IOP Conf. Series: Journal of Physics: Conf. Series **1102** (2018) 012019 doi:10.1088/1742-6596/1102/1/012019

Optimal yaw strategy for optimized power and load in various wake situations

Albert M. Urbán[1], **Torben J. Larsen**[1], **Gunner Chr. Larsen** [1], **Dominique P. Held**[1,2], **Ebba Dellwik**[1], **David Verelst**[1]

[1] Department of Wind Energy, Technical University of Denmark, Frederiksborgvej 399, 4000 Roskilde, Denmark.

[2] Windar Photonics A/S, Helgeshøj Alle 16, 2630 Taastrup, Denmark

Abstract. The interaction between nearby wind turbines in a wind farm modifies the power and loads compared to their stand-alone values. The increased turbulence intensity and the modified turbulence structure at the downstream turbines creates higher fatigue loading, which can be mitigated by wind farm and/or wind turbine control. To alleviate loads and maximize power possible strategies such as wake steering, where the turbine is yawed to redirect the wake such that it does not impinge the downstream turbine, have been studied. The work presented here focuses on situations where the wake is nevertheless affecting the downstream turbine, and more specifically how high loads can be avoided by yawing the wake-affected turbine. The analysis is conducted on a 2.3 MW machine, and the flow field is simulated using the Dynamic Wake Meandering model. The study investigates the impact on power and loads for different longitudinal interspacing and turbulence intensities. Optimal yaw strategies are defined for above rated regions where no power loss occurs. The potential load alleviation for different load sensors are studied, but the presentation is focussed on the blade root flapwise fatigue loading. For full wake at 3D interspacing and turbulence intensity of 5 %, around 35 % of load reduction on the 1 Hz Damage Equivalent Loads can be achieved at high wind speeds. Smaller reductions are achieved for higher atmospheric turbulence; the analogue case with 15 % turbulence intensity shows 17 % potential alleviation. The alleviation on the wind turbine lifetime is also calculated and compared for different turbulence intensities and mean wind speeds. Small reductions are achieved for sites with low mean wind speed and high turbulence intensity, but high reductions, of around 19 %, are accomplished in low turbulence intensity with high mean wind speed.

1. Introduction

The competitiveness on the wind energy market has pushed the wind turbine industry to develop larger rotors, which yield higher power output. The control system of the turbine is also evolving with the inclusion, for example, of lidar systems. The additional information provided by such sensors has the potential to be used by modern control systems to optimize power and/or reduce the wind turbine loading.

Even though the final objective is the same, maximizing power while minimizing loads, different approaches have been presented in the literature. On a single wind turbine, strategies such as individual pitch control for load reduction is studied by [1], where it is demonstrated that a significant reduction in loading can be achieved using relatively straight forward control strategies. Several

modern control strategies, like model predictive control, uses information of the wind field upstream of the turbine and a turbine model to optimize the controller operation set point. The capability of using lidar systems in load reduction and energy yield is shown in [2].

The controller becomes even more complex, when interaction with nearby wind turbines needs to be taken into account. During the operation of a wind farm, full and partial wake situations occur frequently. Wind farm control has been investigated in the last years. In [3], the benefits of wake steering to increase power production and reduce loading on wind farm level are presented.

Yaw control is another interesting option to maximize power and decrease loads. Several studies have addressed the importance of wind turbine alignment in below rated region to optimize power capture. The study in [4] presented the case of a 2.3 MW offshore turbine, where an error on the static yaw calibration leads to a loss of around 0.2% in AEP. Load reduction can also be achieved by active misalignment of an isolated machine. In [5] the load alleviation potential, when vertical shear is present, was studied. The same phenomena is investigated by [6] and compared with field measurements. It was shown that by misaligning turbines in above-rated regime, blade loading can be reduced while maintaining power production. However, the loads on the non-rotating components was increased.

This paper focuses on finding an optimal yaw strategy of a downstream wind turbine under the influence of different wake conditions. First, the methodology is explained describing the setup, characterizing the downstream flow and defining the optimal yaw control strategy. Then, the impact of yawing under different wake condition and its effects on the load level is discussed.

2. Methodology

2.1. Simulation Setup

Power production as well as selected load sensors on the wind turbine are obtained by aero-servo-elastic simulations computed with HAWC2 [7]. The simulated wind turbine is a collective pitch regulated, variable speed turbine with a rotor diameter of 90 m and a rated power of 2.3 MW at 12 m/s. It is using DTU's open-source controller.

Two turbines are used in the setup: the first turbine is used to generate the wake, while the power production and loads are computed on the second turbine, see left panel of figure 1. The unsteady inflow conditions are defined on the upstream turbine. Thus, the downstream turbine feels a disturbance of the original inflow due to the wake. It is important to remark that wake steering by the upstream turbine is not part of this analysis.

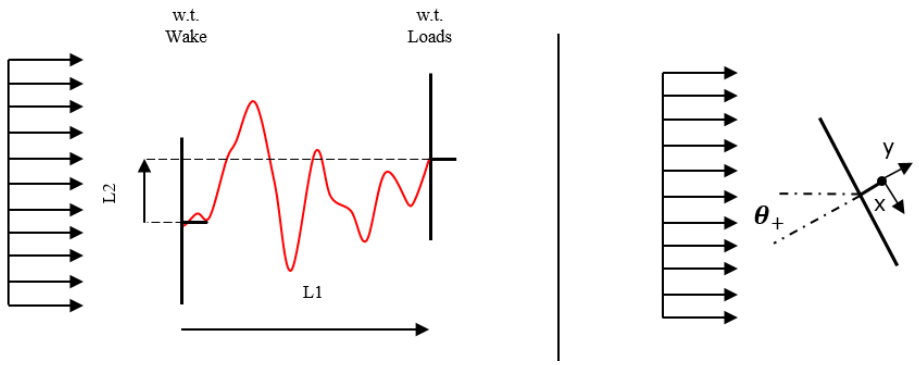

Figure 1: *Left*: Simulation setup with the upstream turbine that is emitting the wake and the downstream turbine where the yaw strategy is applied and the loads are calculated. The red line indicated the movement of the wake. *Right*: Illustration of the turbine yaw convention.

Figure 1 presents the wind turbine configuration, where the left turbine (upstream) is used to generate the wake observed by the right turbine (downstream). L1 corresponds to the longitudinal, along wind speed direction, and L2 relates to the transversal direction. A positive value of L2 corresponds to a displacement of the wake origin to the left as seen from the second turbine facing the mean wind speed direction. The yaw misalignment angle is defined such that a positive angle corresponds to the wind reaching the turbine from the right seen from the turbine, see figure 1.

Normal production, according to IEC 61400-1, is run for a range of yaw misalignments of the downstream wind turbine, where the power and the Damage Equivalent Loads (DELs) of selected channels are computed. In order to cover the variability of the optimal yaw strategy for a wide range of sites, the simulated cases need to cover a large number of scenarios. The investigated scenarios include mean wind speeds ranging from 4m/s to 25m/s in 1m/s steps and turbulences intensities from 5%, to 25% in 5% steps. Six turbulence seeds are used. Further, different discrete yaw scenarios were used, covering a misalignment angle $\theta = \pm 30°$ with 2.5° steps. A power shear law is used with an exponent of 0.2.

2.2. Wake modelling

The upstream wake is simulated using the DWM (Dynamic Wake Meandering) model [8,9], which has been successfully compared to full-scale measurements from the Egmond aan Zee wind farm [10]. The simulated wake deficit and the wake-added turbulence as function of wind speed is shown in figure 2. In the left panels different ambient turbulence levels are studied, while the right panels show the influence of different turbine spacing.

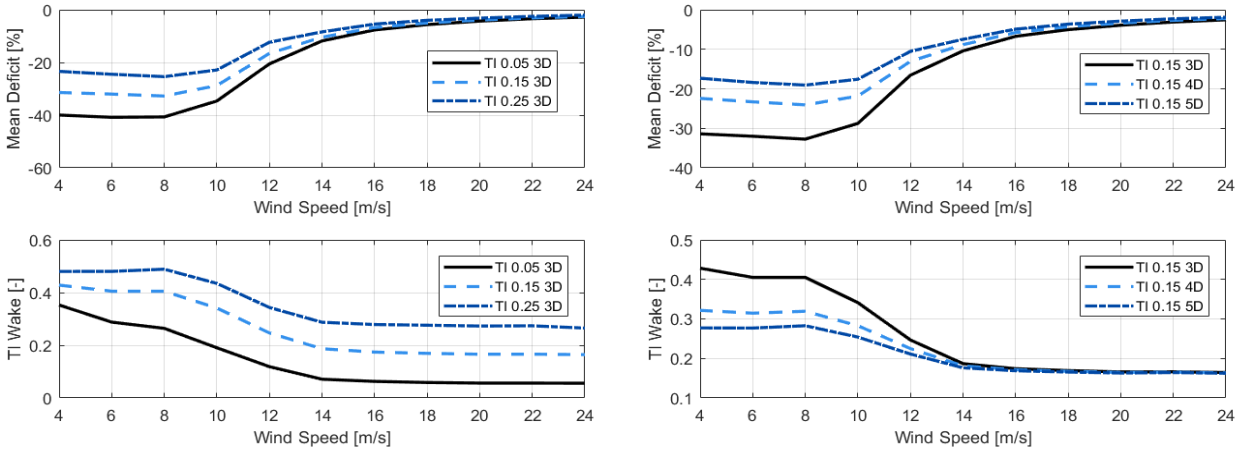

Figure 2: Wake deficit and wake-added turbulence intensity as function of wind speed for different ambient turbulence intensities (*left*) and different turbine spacing (*right*).

The presented values are extracted at the downstream rotor position using the observed wind speed at the rotor plane with a discretization of 1x1 meter and the mean wind speed value over 6 seeds for each wind speed is extracted. The presented results are aligned with the results shown in [8]. The mean inflow deficit is larger for the low turbulence intensities due to the modest mixing of the wake with the undisturbed wind field (figure 2, upper left). The wake recovery is also a function of the distance to the upstream turbine (figure 2, upper right), where the further the distance to the upstream turbine, the lower is the wind speed deficit observed by the wake-affected turbine. The turbulence intensity difference is dependent on both the original level and the wake distance. For identical atmospheric turbulence, the turbulence intensity difference felt by the downstream turbine (fig 2, bottom right) decreases with downstream distance.

An optimal yaw strategy, especially in partial wake situations, depends on the condition that the simulated wake correctly resembles real wake conditions. Thus, it is important to ensure that the wake is meandering in the simulations. HAWC2 provides the wake deficit position resulting from the meandering process. To illustrate the wake meandering effect, the wake center position as function of time was tracked (figure 3). A Cartesian coordinate system with origin at the rotor centre of the downstream turbine is used.

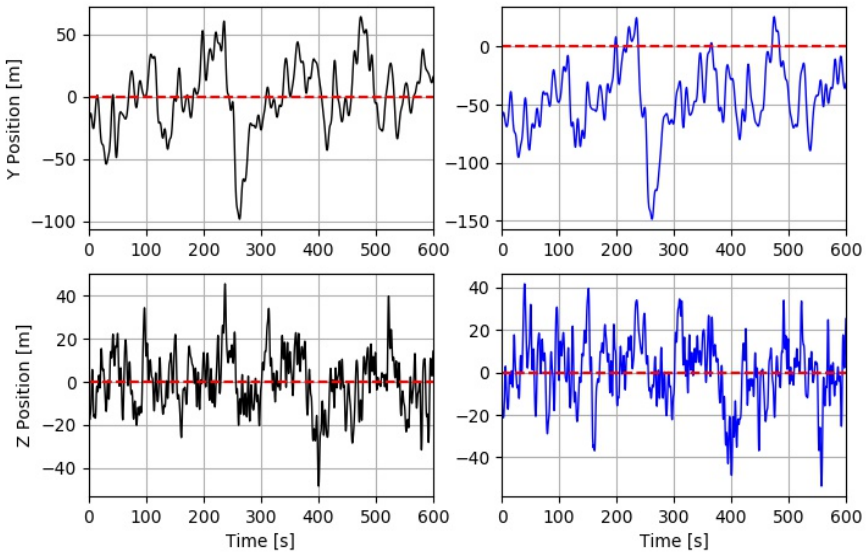

Figure 3 : Wake center position of a full-wake situation (*left*) and a half-wake situation (*right*).

Figure 3 shows a visualization of the wake meander process associated with a full wake case, where the upstream turbine is aligned with the downstream (left figure) and a half wake case (right figure), where the upstream turbine is displaced half diameter (45m) from origin. In both plots, the red line represents the rotor centre of the downstream turbine. Regarding the full wake case, both displacements in y and z have a mean around 0, which implies that the wake meanders symmetrically on the rotor plane. On the other hand, the half wake case presents a negative mean displacement, which corresponds to the half wake. This has an implication on loads and power production, since there is an asymmetry of the mean inflow wind speed on each side of the rotor.

2.3. Yaw control workflow

The implemented method aims to: (1) define a yaw strategy as function of the atmospheric condition and wake position; and (2) to compare the load level to a non-yawed turbine. The output of the workflow results in a yaw strategy for each of the load channels and its associated load alleviation on the lifetime damage of the turbine compared to the non-yawed case. The figures shown in this chapter correspond to a full wake case at 3D and an ambient turbulence intensity of 15%. The mean wind speed is described in terms of a Weibull distribution with 8 m/s mean wind speed and shape factor of 2. The figures are presented to facilitate the explanation of the method.

The data is binned in wind speed and yaw direction, and the annual energy production is obtained. The wind speed frequency values are obtained using a truncated two parameters Weibull distribution. Then, the lifetime damage equivalent loads are calculated using:

$$L_{eq} = \left(\frac{N_{life} \sum_{i=1}^{N} f \, {S_{eq}}^{m}}{N_{eq}} \right)^{m}, \tag{1}$$

where L_{eq} is the lifetime DEL, S_{eq} the mean binned 1 Hz DEL, N_{life} the number of seconds in 20 years lifetime, $N_{eq} = 1e7$ the reference equivalent load and m is the Wöhler exponent. For blades $m = 10$ and for the tower and the shaft $m = 4$.

The optimal yaw control algorithm is constrained such that no power loss is achieved. This is a simplification of a more generalized problem where, in case of the existence of a cost-model, power could be sacrificed, if the value of load reduction is higher than the loss in power production. Thus, the first step is to ensure that the optimal yaw controller operates in maximum power for a given wind speed. The maximum power regime identification is done so that, the maximum power per wind speed is found and subsequently the other values are normalized against that.

$$\Delta P(\theta, v) = \frac{P(\theta, v)}{\max(P(\theta, v))}, \tag{2}$$

where v is the free stream wind speed in the simulation. Thus, the optimal yaw angle θ_{opt} can only be found in regimes where $\Delta P(\theta_n, V_0) = 1$. The power normalization and maximum power regime identification are shown in figure 4.

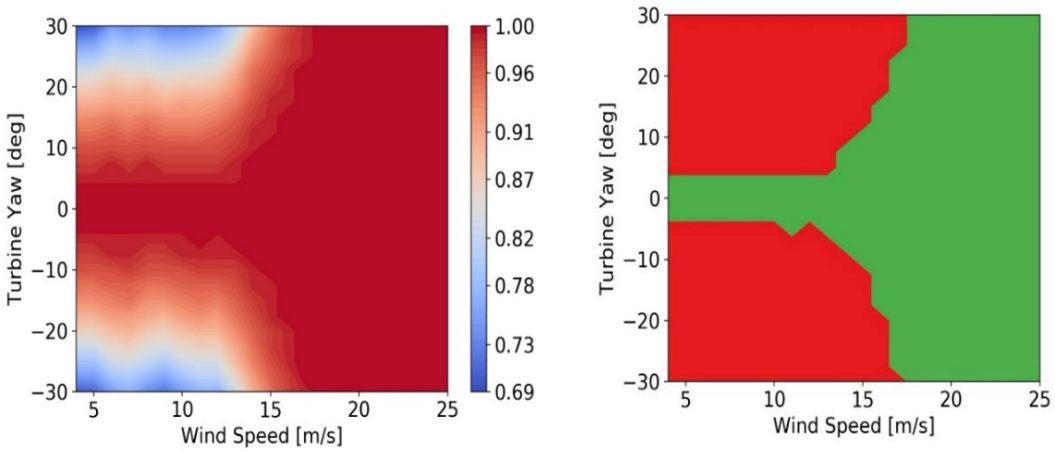

Figure 4: Full wake at 3D from origin and turbulence intensity of 15%. Left: power normalization to the aligned case; Right: region identification for optimal yaw controller.

On the left, it is possible to observe the normalized power as function of wind speed and yaw misalignment. In above-rated wind speed regions large yaw misalignments are possible without power loss. On the right, the regime identification is done based on condition of no power loss.

The 1Hz DEL of blade flapwise bending moment is used to design the yaw optimal controller. In this case, the variation of fatigue loading is normalized against the aligned case $\theta = 0°$:

$$\Delta S(\theta, v) = \frac{S_{eq}(\theta, v)}{S_{eq}(0°, v)}. \quad (3)$$

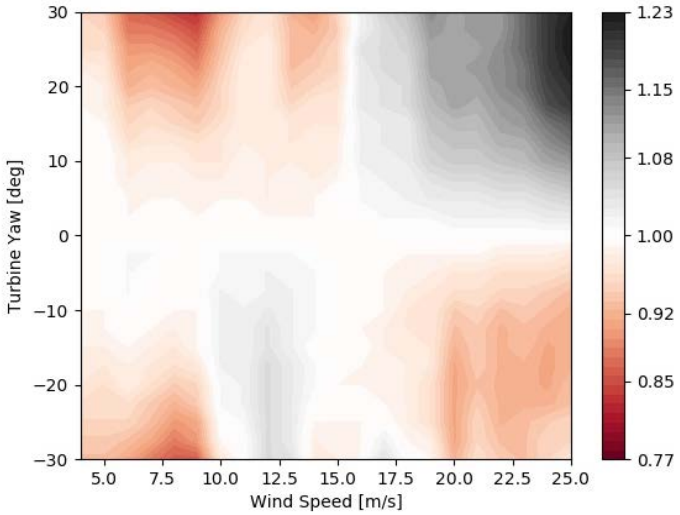

Figure 5: Blade flapwise 1Hz DEL normalized with non-yawed case with wake at 3D from origin and turbulence intensity of 15%.

Figure 5 shows the flapwise blade root 1 Hz DEL as a function of wind speed and turbine yaw. It is observed that the increase of fatigue damage ≅20% for positive angles at high wind speed, while a reduction around ≅ 17% is achieved for negative angles, below rated power. The superposition of the constraint regimes based on power and the fatigue variation provides the information required to define the optimal yaw strategy. The optimal angle, conditioned on mean wind speed, is defined in equation 4:

$$\theta_{opt}(v) = \arg\min_{\theta}\left(\Delta S(\theta, v)\right) \text{ subject to } \Delta P = 1. \quad (4)$$

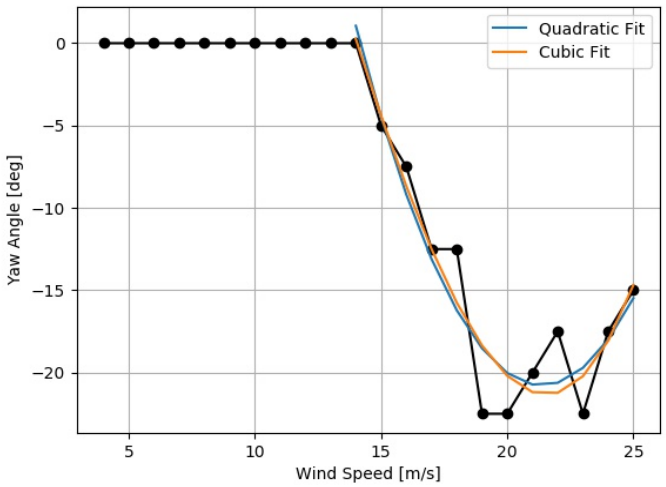

Figure 6 : Optimal yaw angle fit based on blade flapwise bending momment at full wake at 3D from origin and turbulence intensity of 15%.

The result of the blade flapwise yaw strategy can be observed in figure 6. The used discretization, 1 m/s for wind speed and 2.5° on yaw, is enough to provide a rough visualization on the yaw angle, but it is however found too course to define a strategy, which could be implemented in a control system. The discrete optimal angle distribution is used to fit a quadratic and cubic expression.

The fit is evaluated for each wind speed, and compared to the original discrete controller fatigue reduction. In this case, the mean squared error, MSE, between the original yaw angle and the fitted, is not relevant for this analysis. Instead, it is important to evaluate the difference on the 1 Hz damage equivalent. The controller is considered correctly fitted, if the error on the 1 Hz damage equivalent load for all wind speeds is smaller than 0.5 %.

3. **Results**

3.1. Load reduction

The lifetime DEL is presented for the normal operation case, where the wind turbine is aligned with the wind, see table 1. Different upstream wind turbine spacing and position cases are presented and the values are normalized to the un-waked case to determine the increase of lifetime loading due to wake (ΔW). Table 1 presents an example of the blade flapwise lifetime DEL for different upstream wake positions.

Table 1: Lifetime DEL increase comparison for ambient turbulence intensity 15 % and Weibull parameter A=8 m/s k=2.

Channel	Case	ΔW[%]
Blade Flapwise	Reference 0.15	100
	3D 0.15	110.5
	4D 0.15	109.1
	5D 0.15	107.7
	3D 0.15 +0.5D	117.6
	3D 0.15 -0.5D	110.1

The lifetime DEL is increased with decreased distance to the upwind turbine. An asymmetry can be found in the partial wake cases - positive displacement on the perpendicular direction of the wake deficit presents higher loading than negative, which can be explained by the tilt angle combined with the wake deficit and shear.

Once the increment of loading due to the wake is presented, the potential fatigue DEL reduction is evaluated for several load channels. Here the blade flapwise bending moment (BF), the blade edgewise bending moment (BE), the tower top fore-aft bending moment (TT Fa) and the tower top side-side bending moment (TT Ss) are compared. An example for $v = 18$ m/s, TI=15% is shown in figure 7.

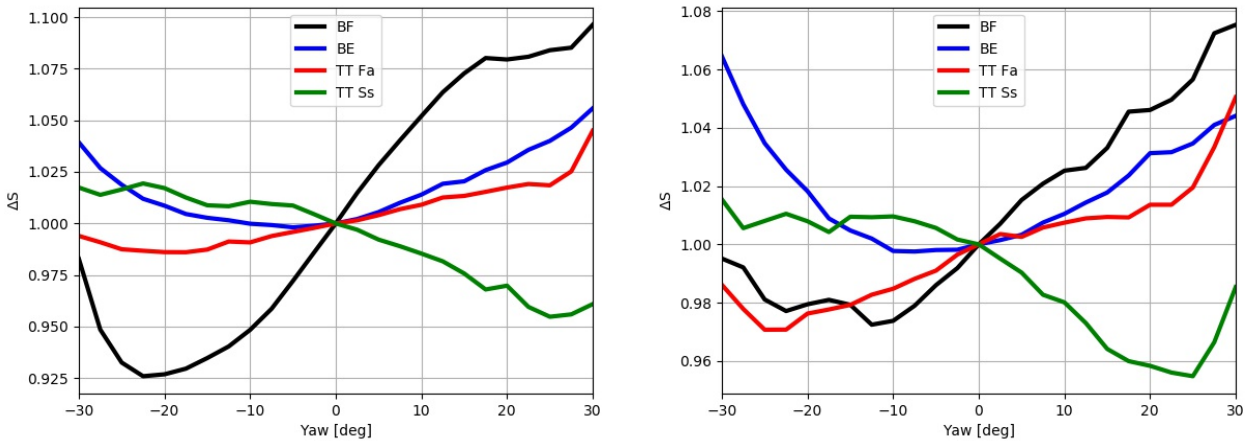

Figure 7: Load variation as function of yaw misalignment for a non-wake case (left) and a wake at 3D (right) at an TI of 15% at mean upstream wind speed of 18 m/s .

It can be seen that the BF is reduced in both cases when negative yaw misalignments are applied. For the non-wake case reductions around 7.5% are achieved at a misalignment of 22°. The reduction is lower in a waked case. There is a small increase for TT Ss and BE towards negative angles.

In general, lower TI will yield a higher load alleviation because the loads are dominated by the shear. For the lowest simulated TI = 5% at 14 m/s a 35% reduction was achieved at high wind speed and large yaw misalignment.

3.2. Optimal yaw strategy

The wind turbine yaw controller was defined as the setting that resulted in minimized blade flapwise fatigue loads. Four different yaw strategies corresponding to different turbine positions are presented in figure 8 using the same background atmospheric turbulence intensity of 15%.

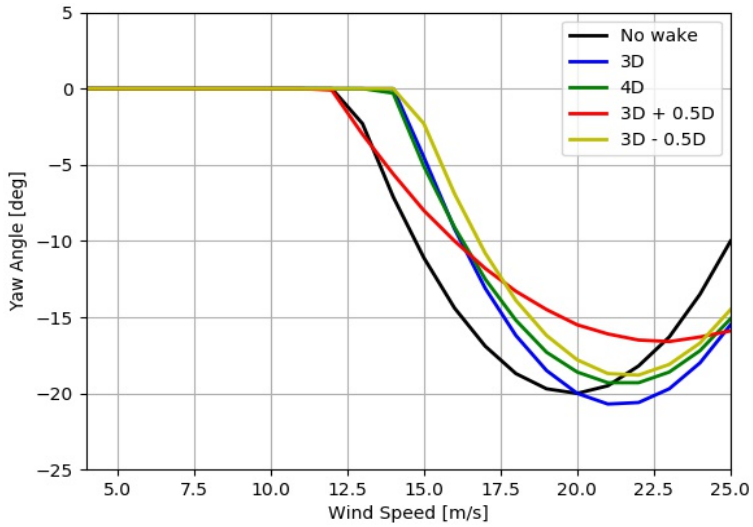

Figure 8: Yaw control strategy comparison for different wake positions for ambient turbulence intensity at 15%.

For all upstream turbine positions the optimal yaw angle is negative. The yaw controller starts acting at different wind speeds depending on where equation 4 is fulfilled. Thus, for the case without a wake (black curve) it is possible to define a yaw strategy that starts around 12 m/s, whereas for the 3D spacing case, the strategy starts around 14 m/s. The maximum yaw angle is found to be similar for the case without wake, the 3D and the 4D case, around -20 degrees. The partial wake scenarios results are different due to the asymmetry of the wake impact. It is also important to consider the effect on other load channels.

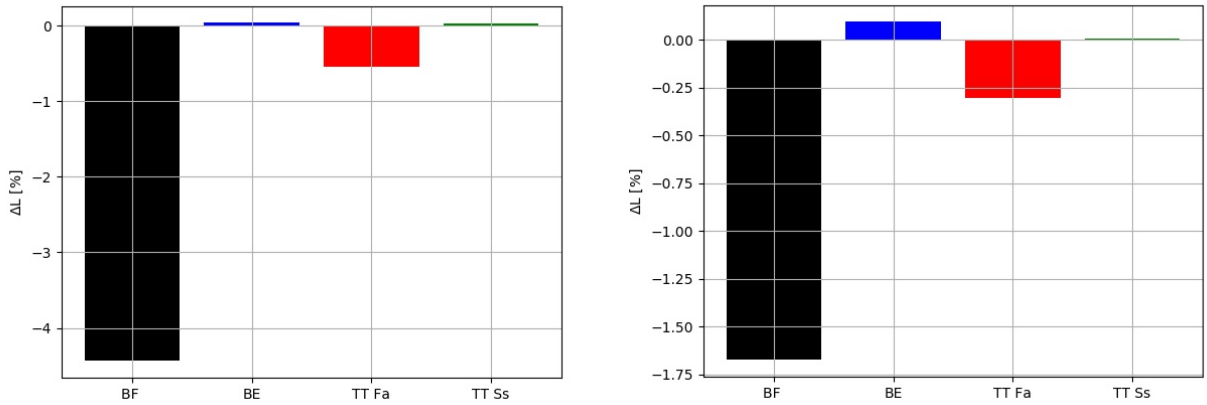

Figure 9: Lifetime DEL using the optimal yaw controller for a non-wake case (left) and a waked case (right) at TI of 15%, Weibull parameter $A = 8$ m/s and $k = 2$

In figure 9 the lifetime DEL reduction is presented using the optimal yaw strategy. It is shown that BF loads are alleviated. The reduction is smaller for wake cases because the wake add additional loading, which cannot be reduced by yawing, see table 1. The reduction achieved ranges from -4.5 % for the free inflow condition case to -1.7 % for the full wake case. Slight increases for BE and TT Ss can be observed. The results are dependent on the used Weibull distribution, and the discussion follows in the next section.

The loading and optimal yaw control strategy is depending on TI. The optimal controller for different turbulence intensities is shown in figure 10 and its reduction appear in table 2.

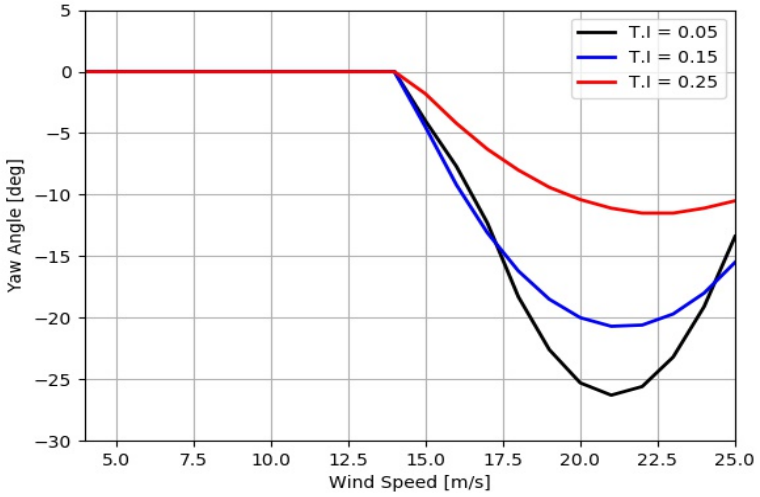

Figure 10: Yaw control strategy comparison for full wake at 3D and different ambient turbulence intensities.

Table 2: Lifetime DEL and reduction comparison for full wake at 3D and different ambient turbulence intensities.

Channel	Case	Lifetime DEL comparison [%]	ΔL using $\theta_{opt}(v)$ [%]
Blade Flapwise	3D 0.25	100 %	-1.4 %
	3D 0.15	69.5 %	-1.7 %
	3D 0.05	32.4 %	-7.8 %

The optimal yaw control strategies achieve higher peak values the lower the turbulence intensity is. The lifetime reduction value is higher, 7.8 %, for the lower turbulence intensity.

3.3. Sensitivity to Weibull distribution

The yaw controller performance is evaluated, in this paper, by comparing the lifetime DEL reduction to its value in normal operation. Another possibility is to compare the 1 Hz fatigue loading for the operating wind speeds. This procedure is discarded, since it requires a large number of information to evaluate the controller performance if more than one inflow condition is compared.

By using the lifetime load value, the wind speed probability density function needs to be included, as defined in equation 1. The yaw controller is independent on the wind probability, since it minimizes the 1 Hz damage equivalent load as function of wind speed. However, the reduction results provided in table 1 and 2 depends on the probability distribution. The Weibull distribution is changed to analyze the load reduction sensitivity to the applied Weibull distribution. The shape factor remains constant, k = 2, for the three Weibull intensity parameter choices, where the mean wind speed is changed to 6 and 12, respectively. The reduction is calculated, considering the lifetime value for each Weibull distribution, and presented in tables 3 and 4.

Table 3: Lifetime reduction comparison for ambient turbulence intensity 15 % and Weibull distributions with k =2 and A = 6, 8 and 12 m/s.

Channel	Case	ΔL using $\theta_{opt}(v)$, A= 6 [%]	ΔL using $\theta_{opt}(v)$, A= 8 [%]	ΔL using $\theta_{opt}(v)$, A= 12 [%]
Blade Flapwise	Reference 0.15	-1.12 %	-4.5 %	-7.75 %
	3D 0.15	-0.3 %	-1.7 %	-5.8 %
	4D 0.15	-0.3 %	-2.0 %	-6.6 %
	5D 0.15	-0.2 %	-2.1 %	-6.7 %
	3D 0.15 +0.5D	-1.0 %	-1.9 %	-5.6 %
	3D 0.15 -0.5D	-0.1 %	-1.2 %	-5.1 %

Table 4: Lifetime reduction comparison for full wake at 3D and different ambient turbulence intensities and Weibull distribution with k =2 and A = 6, 8 and 12 m/s.

Channel	Case	ΔL using $\theta_{opt}(v)$, A= 6 [%]	ΔL using $\theta_{opt}(v)$, A= 8 [%]	ΔL using $\theta_{opt}(v)$, A= 12 [%]
Blade Flapwise	3D 0.25	-0.1 %	-1.4 %	-2.2 %
	3D 0.15	-0.3 %	-1.7 %	-5.8 %
	3D 0.05	-1.9 %	-7.8 %	-19.5 %

For Weibull distributions with predominance of lower wind speeds, A = 6 m /s, the reductions obtained are lower than for the distributions with higher mean wind speed. The designed controller operates mainly in above-rated conditions, guarantying power production, thus not reducing fatigue loading in the partial load regime.

4. Conclusion and future work

The fatigue load potential reduction is investigated in this study and a simple method for defining the optimal yaw strategy for a wind turbine affected by wake from an upstream turbine. The defined strategies can be implemented in the wind turbine control system where, for example, lidars can be used to detect the presence of the wake in the approaching flow as demonstrated by [11,12].

In previous studies the accuracy of inflow measurements by nacelle lidar systems have been investigated. Intercomparisons with sonic anemometers showed very good correlation and no biases of the mean wind speeds. Similarly, turbulence intensity measurements can be achieved through the calculation of average Doppler spectra. The ability to detect wakes is shown in [12]. There, the spectral width of the Doppler spectra is used to determine small-scale turbulence levels. Comparing these levels to ones measured during wake-free situations, it is possible to identify instances where a wake is impinging the inflow.

The simulations carried out with HAWC2 for the aero-servo-elastic model and DWM for the wake modelling has been conducted on a 2.3 MW machine. The defined yaw controller is constrained to achieve maximum power, thus, operating in the above-rated condition where the inclusion of yaw misalignment does not alter the rated power. The optimal yaw controller could be applied more broadly in below rated conditions, to further alleviate the high wake loads, for example, by applying a cost model.

The flapwise fatigue loading is presented in this paper, showing load alleviation towards negative yaw angles. The optimal yaw strategy presented in figure 8 and figure 10 depends on the inflow conditions. For the same atmospheric turbulence intensities, the controller presents a similar pattern but shifted towards the highest wind speed for low interspacing. An exception is found in one of the partial wake cases, 3D and ½ D lateral displacement. The wake asymmetry and the effect on tilt angle will be investigated in future papers. For the same spacing, but different turbulence intensities, the lower the turbulence intensity, the higher the value of the optimal yaw controller.

Low turbulence intensity sites have a larger potential for load alleviation. For example, a 35 % load reduction in the 1 Hz flapwise DEL is observed for high wind speeds at 3D full wake at 5 % turbulence intensity. The higher the turbulence intensity is, the smaller the potential load reduction is. The lifetime damage equivalent load is computed for three different mean wind speed sites,

concluding that the highest potential load alleviation is found in cases with low turbulence intensity and high mean wind speed. The presented values do not take into account the operating frequency of the various wake conditions. Turbine and site specific reductions are found dependent on the park layout, machine and wind distribution.

The sensitivity of shear is not included in this paper even though the load reduction is depending on it, since it produces a once-per-revolution variation. In future work, one dimension will be added to the analysis to study the importance of the combined effect of shear and wake.

The investigation of the optimal yaw controller at partial wake should be extended to cover more wake positions than half-wake and full-wake. Also, the half-wake situations in this paper are not guaranteed to only affect half of the rotor, since the dynamic wake meandering model adds a random component to the position of the wake.

5. Acknowledgements

This research was supported by the EUDP funding agency through the project Lidar detection of wakes for wind turbine optimization.

6. References

[1] E. A. Bossanyi, “Individual blade pitch control for load reduction,” *Journal of Wind Energy* 2003, **6**: 119–128.

[2] D. Schlipf, “Lidar-Assisted Control Concepts for Wind Turbines,” PhD-thesis, Faculty of Aerospace Engineering and Geodesy of the University of Stuttgart (2015).

[3] P. Flemming et. al, “A simulation study demonstrating the importance of large-scale trailing vortices in wake steering,” Wind Energy Science 2018, **3**: 243-255

[4] K. A. Kragh and M. H. Hansen, “Potential of power gain with improved yaw alignment,” Wind Energy 2015; **18**:979-989

[5] K. A. Kragh and M. H. Hansen, “Load alleviation of wind turbines by yaw misalignment,” Wind Energy 2014; **17**:971-982

[6] R. Damiani et.al, “Assessment of Wind Turbine Component Loads Under Yaw-Offset Conditions,” Wind Energy Science 2017; **3**: 173–189

[7] T. J. Larsen and A. M. Hansen, “How 2 HAWC2, the user’s manual,” Tech. Rep., 2007.

[8] G. C. Larsen et. al., ”Wake meandering: a pragmatic approach,” Wind Energy 2008; **11**(4): 377–395

[9] H. Aa. Madsen et. al., “Calibration and validation of the dynamic wake meandering model for implementation in an aeroelastic code,” Journal of Solar Energy Engineering 2010; **132**(4): 041014

[10] T. J. Larsen et. al. ”Validation of the dynamic wake meander model for loads and power production in the Egmond aan Zee wind farm” Wind Energy 2013; **16**:605-624

[11] T G Herges et. al. ”Detailed analysis of a waked turbine using a high resolution scanning lidar,” The Science of Making Torque from Wind, J. Phys.: Conf. Ser. 2018; **1037**: 072009

[12] D. P. Held et al. ”Wake detection in the turbine inflow using nacelle lidars,” in review